

CHIRAL SYMMETRY BREAKING AND THE PION

V. Bernard, R. Brockmann, W. Weise and E. Werner
Institute of Theoretical Physics
University of Regensburg
D - 8400 Regensburg, W. Germany

1. Introduction

The special properties of the pion (in particular: its small mass) are frequently interpreted as being related to chiral symmetry and its spontaneous breaking. Approximate chiral symmetry manifests itself in various ways in nuclear and low energy particle physics (through PCAC, the Goldberger-Treiman relation, the low energy theorems in pion-nucleon scattering etc.). Chiral bag models¹⁻³⁾ use this concept to surround the quark core with a (massless) pion field, the Goldstone pion, coupled to the bag boundary such that the axial current becomes continuous at the boundary.

However, the pion in this model is a pointlike, structureless object. There is no obvious relationship to an underlying $q\bar{q}$ -structure in this picture. The only reference to intrinsic pion properties is in terms of one (phenomenological) parameter, the pion decay constant $f_\pi = 93$ MeV.

The motivation of the present work is to investigate the connection between the Goldstone Boson nature and the quark-antiquark structure of the pion. We shall adapt the Nambu and Jona-Lasinio (NJL) chiral symmetry breaking scheme⁴⁾ to hadrons of finite size. This will be based on an effective Hamiltonian^{5,6)} which combines the underlying chiral symmetry of QCD for massless quarks with the phenomenology of confinement at hadronic length scales and asymptotic freedom at short distances.

The result is the pion as a (highly collective) superposition of $q\bar{q}$ -states with a strongly reduced $q\bar{q}$ valence quark content. A test of the intrinsic pion wave function is provided by a calculation of the $\pi^\pm \rightarrow \mu^\pm \nu$ decay. Finally, a few related topics will be discussed, such as the role of the pion cloud in the nucleon charge and axial form factors.

2. Chiral Symmetry and Bag Model Phenomenology

As a starting point, consider the fundamental QCD Lagrangian L_{QCD} in the flavour SU(2) sector. For massless up and down quarks, $m_u = m_d = 0$, L_{QCD} is invariant under the chiral SU(2) x SU(2) transformation of the quark fields:

$$\psi \rightarrow \exp [i \gamma_5 \vec{\tau} \cdot \vec{\Theta}] \psi, \quad \bar{\psi} \rightarrow \bar{\psi} \exp [i \gamma_5 \vec{\tau} \cdot \vec{\Theta}]. \quad (1)$$

Equivalently, the quark axial current

$$A_\lambda^\mu(x) = \bar{\psi}(x) \gamma^\mu \gamma_5 \frac{\tau_\lambda}{2} \psi(x), \quad (2)$$

is a conserved quantity, i.e. $\partial_\mu A^\mu = 0$.

On the other hand, the non-linear self-couplings of the gluonic part of L_{QCD} are supposed to create confinement for colored objects such as individual quarks. The act of confinement necessarily implies a breaking of chiral symmetry at the quark level (dynamical symmetry breaking). This can be illustrated as follows: assume that the confining forces generate a scalar confining potential (or local mass) $M(x)$ for individual quarks inside the hadron. The single particle Dirac equation is

$$[i \gamma_\mu \partial^\mu - M(x)] \psi = 0 \quad (3)$$

Consequently, the divergence of the quark axial current becomes

$$\partial_\mu [\bar{\psi} \gamma^\mu \gamma_5 \frac{\tau_\lambda}{2} \psi] = M(x) \bar{\psi} i \gamma_5 \tau_\lambda \psi \equiv J_{5\lambda} \quad (4)$$

In bag models, the confining potential is replaced by a sharp boundary condition, in which case $J_{5\lambda}$ becomes proportional to a δ -function at the bag radius.

The non-vanishing divergence of the axial current measures the degree to which chiral symmetry is broken, at the quark level, in terms of a pseudoscalar-isovector source function $J_{5\lambda}$. In chiral bag models^{2,3)}, this $J_{5\lambda}$ is interpreted as the (surface peaked) source function of the Goldstone pion, introduced such as to restore chiral symmetry. As mentioned before, the pion in such models is an elementary field, without any reference to an underlying $q\bar{q}$ substructure.

Chiral bag models have established successful phenomenology in several respects: they provide a simple model of pion-nucleon coupling; they reproduce basic chiral symmetry and current algebra results such as the Goldberger-Treiman relation; and they permit to obtain a certain amount of consistency with nuclear physics and the long range properties of the nucleon-nucleon interaction, by allowing for quark core radii considerably smaller than in the original MIT bag, and by generating the appropriate one-pion exchange potential between separated bags.

An apparently unrelated picture of the pion is that of a single $q\bar{q}$ pair in the lowest orbit of a bag or confining potential (we refer to this as the bag model pion). This bag model pion usually comes out much too heavy, except for the question of (ambiguous) center-of-mass corrections.

3. Chiral Effective Lagrangian

In trying to establish a connection between the Goldstone pion and the $q\bar{q}$ pion, we wish to construct a suitable effective Lagrangian which combines features expected from QCD with the underlying chiral symmetry .

We start again from the chiral invariant QCD Lagrangian L_{QCD} in the flavour SU(2) sector with current quark masses $m_u = m_d = 0$. We assume that the gluonic degrees of freedom can formally be eliminated from L_{QCD} without breaking its chiral SU(2) x SU(2) symmetry. This leads to the replacement of L_{QCD} by a chiral invariant effective Lagrangian in which an effective quark-quark interaction is the remnant of the non-linear gluon dynamics.

The assumed "minimal" effective action is:

$$S = \int d^4x \bar{\psi}(x) i\gamma_\mu \partial^\mu \psi(x) + \int d^4x_1 \dots d^4x_4 K(x_1 \dots x_4) [\bar{\psi}(x_1)\psi(x_2)\bar{\psi}(x_3)\psi(x_4) + \bar{\psi}(x_1)i\gamma_5\vec{\tau}\psi(x_2) \cdot \bar{\psi}(x_3)i\gamma_5\vec{\tau}\psi(x_4)]. \quad (5)$$

The interaction kernel K cannot be calculated from first principles; however, it must be consistent with certain features derived from or suggested by QCD:

- (a) The kernel K cannot only depend on space-time distances between quarks. This is a natural consequence of the elimination of the gluonic degrees of freedom: since the gluonic fields have their own dynamics, their elimination manifests itself in the form of a distinguished reference frame. Therefore, if the original gluon field was centered at some space time point x_0 , the quark-quark interaction should depend on the distance of each quark relative to x_0 .
- (b) Due to the asymptotic freedom properties of QCD the interaction strength must be weak at small distances so that quarks move essentially freely in the deep interior of hadrons.
- (c) At distances comparable to hadron dimensions a rapid transition from weak to strong coupling sets in. This is suggested by recent Monte Carlo calculations on the lattice.

4. Model Hamiltonian for bound Quark-Antiquark Pairs

We now introduce a model Hamiltonian which has the properties discussed above and allows to demonstrate explicitly the connection between the $q\bar{q}$ -pion and the Goldstone pion. The following simplifying assumptions will be made:

- (i) The interaction part of the Hamiltonian is assumed to be static.
- (ii) The static kernel is represented in the form

$$K = d(\vec{r}_1 \dots \vec{r}_4; \vec{x}_0) \prod_{i=1}^4 G(|\vec{r}_i - \vec{x}_0|)^{1/4}, \quad (6)$$

in such a way that K is invariant with respect to simultaneous translations of any one of the variables \vec{r}_i and \vec{x}_0 .

Here $G(|\vec{r} - \vec{x}_0|)$ is a coupling strength which depends on the distance between the posi-

tion of each quark and the supposed center x_0 of the multigluon field. Furthermore $d(\vec{r}_1 \dots \vec{r}_4; \vec{x}_0)$ is a distribution function. Localizing the kernel in the variables $\vec{r}_i - \vec{r}_j$ (where $i = 1, 2; j = 3, 4$) and identifying the center-of-mass of the interacting quarks with the center x_0 , one obtains the following Hamiltonian $H = H_0 + H_{int}$ (with $x_0 = 0$):

$$\begin{aligned} H_0 &= \int d^3r \bar{\psi}(\vec{r}) \vec{\gamma} \cdot \vec{p} \psi(\vec{r}) \\ H_{int} &= - \int d^3r d^3r' G(r) \delta^3(\vec{r} + \vec{r}') [\bar{\psi}(\vec{r}) \Gamma \psi(\vec{r}') \bar{\psi}(\vec{r}') \Gamma \psi(\vec{r}) \\ &\quad + \bar{\psi}(\vec{r}) \Gamma \psi(\vec{r}') \bar{\psi}(\vec{r}') \Gamma \psi(\vec{r})], \end{aligned} \quad (7)$$

where $\Gamma = 1, i\gamma_5 \vec{\tau}$. We wish to apply it to the description of a bound $q\bar{q}$ pair with zero total momentum, with the center of mass localized at the origin. That is, in Eq. (7), $\vec{p} = -\frac{i}{2} \vec{\nabla}$, where the gradient is taken with respect to \vec{r} , the position of each individual quark with respect to the center.

The interaction H_{int} contains as an essential ingredient the position dependent coupling strength $G(r)$. Following the discussion in section 3, $G(r)$ should become small as $r \rightarrow 0$, while at values of r approaching hadronic dimensions $G(r)$ should increase rapidly.

The model is a natural extension of the Nambu-Jona-Lasinio (NJL) model of chiral symmetry breaking⁴⁾ to a situation where the coupling strength becomes position dependent.

5. Self-consistent Confining Mean Field

In order to obtain the selfconsistent confining potential experienced by each quark we add and subtract a term $M(r)\bar{\psi}(\vec{r})\psi(\vec{r})$ in the Hamiltonian (7). In analogy with the NJL model, $M(r)$ is obtained by linearisation:

$$M(r) = \frac{5}{4} G(r) \text{tr} \langle \psi(\vec{r}) \bar{\psi}(\vec{r}) \rangle, \quad (8)$$

where use has been made of the reflection property $\psi(\vec{r}, \bar{\psi}(\vec{r}) = \psi(-\vec{r})\bar{\psi}(-\vec{r})$. In the factor 5/4 in eq. (8), 1/4 comes from the exchange term of H_{int} eq. (7), after Fierz rearrangement.

The selfconsistency of the procedure requires that the quark fields $\psi(\vec{r})$ have to be evaluated using the Dirac equation

$$[\vec{a} \cdot \vec{p} + BM(r)] \psi(\vec{r}) = E \psi(\vec{r}). \quad (9)$$

(The role of nonzero current quark masses will be discussed later.) The quark fields can be expanded in terms of particle and antiparticle solutions of eq. (9):

$$\psi(\vec{r}, t) = \sum_{\alpha} [u_{\alpha}(\vec{r}) e^{-iE_{\alpha}t} b_{\alpha} + v_{\alpha}(\vec{r}) e^{iE_{\alpha}t} d_{\alpha}^{\dagger}] \quad (10)$$

where b_{α} and d_{α}^{\dagger} are quark annihilation and antiquark creation operators; $\alpha = (nljm)$ denotes quark orbit quantum numbers. One obtains

$$\langle \psi(\vec{x}) \bar{\psi}(\vec{x}) \rangle = \frac{n_f}{2} \sum_{\alpha} [u_{\alpha}(\vec{x}) \bar{u}_{\alpha}(\vec{x}) - v_{\alpha}(\vec{x}) \bar{v}_{\alpha}(\vec{x})] \quad (11)$$

where n_f is the number of flavours.

In order to make the sum over α meaningful one needs a physically motivated cutoff procedure. For this purpose we choose a finite model space to obtain solutions of eq. (8). Subsequent conclusions about the Goldstone boson nature of the pion are independent of the size of this space. With the conventions for the upper and lower components g and f , respectively, of u_{α} and v_{α} defined in ref. ^{5,6}, eq. (8) becomes

$$M(r) = \frac{5}{4} n_f G(r) \sum_{n\ell j} \frac{2j+1}{4\pi r^2} [g_{n\ell j}^2(r) - f_{n\ell j}^2(r)]. \quad (12)$$

Since $G(r)$ is not well known from first principles, we turn the argument around and start with a confining potential $M(r)$ roughly compatible with the systematics of hadron sizes and spectroscopy and calculate $G(r)$ selfconsistently from eq. (12) once a model space is specified.

Potentials of the form $M(r) = cr^n$, $n = 2, 3$ have been used quite successfully to describe various properties of the quark core in nucleons, like electromagnetic ⁷⁾ and axial ⁸⁾ form factors.

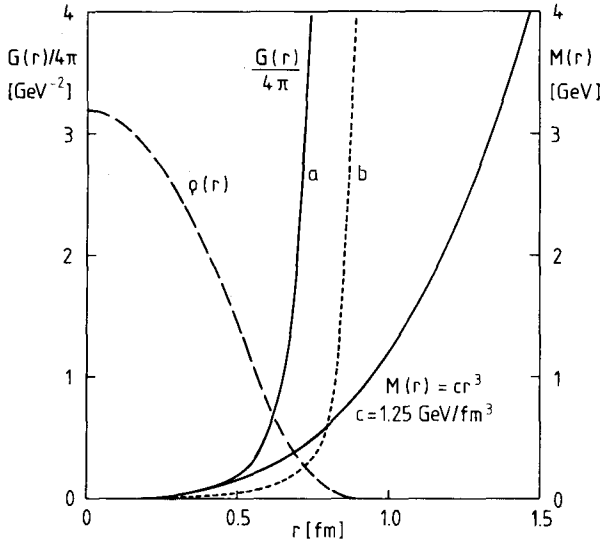


Figure 1: Coupling strength $G(r)$ which generates a confining potential $M(r)=cr^3$ self-consistently, as determined by the mass equation, eqs. (8,12) Curves a and b show results for different model spaces: all $\{1s\ 1/2, 1p\ 3/2, 1p\ 1/2\}$ quark and antiquark orbits (curve a); large space with all $\{1s, 1p, 1d, 2p, 1f\}$ orbits (curve b). Also shown for orientation is the $1s\ 1/2$ quark density distribution.

A typical result is presented in fig. 1 for $n = 3$. The coupling strength $G(r)$ which generates $M(r)$ selfconsistently is shown for two different model spaces. One sees clearly the rapid transition from weak to strong coupling which takes place in the hadron surface.

6. Pion Mass and Wave Function

The effective Hamiltonian developed in the preceding sections will now be used in the $q\bar{q}$ -channel carrying pion quantum numbers. We construct properly coupled eigenfunctions of the Hamiltonian

$$H^{(0)} = -\frac{i}{2} (\vec{\alpha}_1 - \vec{\alpha}_2) \cdot \vec{V} + (\beta_1 + \beta_2)M(r) \quad (13)$$

for $q\bar{q}$ -pairs bound in the confining potential $M(r)$. Note that this effectively introduces confinement in the relative coordinate of the pair. We define basis states $|(q\bar{q})_{\alpha\beta}^+ \rangle = b_{\alpha}^+ d_{\beta}^+ |0\rangle$ for quark and antiquark in orbitals α and β . The corresponding r -space amplitude coupled to total angular momentum J , with center of mass fixed at the origin, is

$$\chi_{\alpha\beta}^J(\vec{r}) = [u_{\alpha}(\vec{r}) \bar{v}_{\beta}(-\vec{r})]^J \quad (14)$$

and satisfies

$$\text{tr}[\chi_{\alpha\beta}^+ H^{(0)} \chi_{\alpha\beta}] = (E_{\alpha} + E_{\beta}) \text{tr}[\chi_{\alpha\beta}^+ \chi_{\alpha\beta}] . \quad (15)$$

The lowest states coupled to $J^{\pi} = 0^{-}$ are $(1s^{1/2})^2$, $(1p^{3/2})^2$, $(1p^{1/2})^2$, the lowest energy being about 600 MeV. The mechanism which brings the energy down to zero is provided by the residual interaction in the pseudoscalar-isovector channel. It is useful to introduce the amplitude

$$D_{\alpha\beta}(r) = \langle (q\bar{q})_{\alpha\beta} | \bar{\psi}(\vec{r}) i\gamma_5 \tau_3 \psi(-\vec{r}) | 0 \rangle \quad (16)$$

where we consider for convenience neutral $q\bar{q}$ -pairs. It is decisive to restrict the space $\{\alpha, \beta\}$ to the model space used for determining $M(r)$. The sum of the direct and exchange matrix elements of H_{int} , eq. (7), is:

$$W_{\alpha\beta, \gamma\delta} = -\frac{5}{2} \int d^3r D_{\alpha\beta}(r) G(r) D_{\gamma\delta}(r) . \quad (17)$$

The eigenvalue equation for the pionic mode can be obtained from the Bethe-Salpeter equation for the amplitude $\phi(x_1, x_2)$ for finding a $q\bar{q}$ -pair at the space-time positions x_1 and x_2 , respectively, within a pion. (It is related to χ , eq. (14), by $\phi = i[\text{tr } \gamma_5 \chi]$). Since our effective interaction is not retarded the Bethe-Salpeter equation reduces to a Salpeter equation. Expanding the intermediate $q\bar{q}$ -propagator in terms of the bound state pairs $(\alpha\beta)$ one arrives at the equation

$$(E_N^2 - E_{\alpha\beta}^2) C_{\alpha\beta}^N = 2E_{\alpha\beta} \sum_{\gamma\delta} W_{\alpha\beta, \gamma\delta} C_{\gamma\delta}^N , \text{ where}$$

$$E_{\alpha\beta} = E_{\alpha} + E_{\beta}, \quad C_{\alpha\beta}^N = X_{\alpha\beta}^N + Y_{\alpha\beta}^N , \quad (18)$$

$$X_{\alpha\beta}^N = \langle 0 | d_\beta b_\alpha | \pi_N \rangle, \quad Y_{\alpha\beta}^N = \langle 0 | b_\alpha^+ d_\beta^+ | \pi_N \rangle.$$

The modes $|\pi_N\rangle$ can be expressed by the amplitudes X and Y: the creation operator Q_N^+ for the mode $|\pi_N\rangle$ defined by $|\pi_N\rangle = Q_N^+ |0\rangle$ is

$$Q_N^+ = \sum_{\alpha\beta} [X_{\alpha\beta}^N b_\alpha^+ d_\beta^+ - Y_{\alpha\beta}^N d_\beta b_\alpha]. \quad (19)$$

Eq. (18) is identical to the well-known RPA equations in many-body physics. The Goldstone boson nature of the pion has been investigated in a model space consisting of all 1s and 1p quark and antiquark orbitals. We find the Goldstone mode at $E = 0$ independent of the value of the potential parameter c in $M(r) = cr$.

We now discuss the effect of finite, but small quark masses $m_1, m_2 = m_u$ or m_d , which adds $\beta_1 m_u + \beta_2 m_d$ in $H^{(0)}$ of eq. (13). This results in the replacement $E_{\alpha\beta} \rightarrow E_{\alpha\beta} + \eta_{\alpha\beta} (m_u + m_d)$, where $\eta_{\alpha\beta}$ is determined to be close to 0.6 for the model considered here, almost independent of the quark single particle orbits.

This induces a first order change ΔE of the Goldstone mode given by

$$(\Delta E)^2 = \frac{\sum_{\alpha\beta} E_{\alpha\beta} C_{\alpha\beta} \eta_{\alpha\beta}}{\sum_{\alpha\beta} C_{\alpha\beta}} (m_u + m_d) \quad (20)$$

The resulting relationship between the pion mass $m_\pi = \Delta E$ and the current quark masses is of the same functional form as obtained from current algebra and QCD sum rules⁹⁾, namely $m_\pi^2 = \text{const.} (m_u + m_d)$. The numerical calculations reproduce the empirical pion mass for $m_u + m_d$ between 30 and 40 MeV, depending moderately on the size parameter c of the confining potential. The quadratic relationship between m_π and $m_u + m_d$ is reproduced with an extremely good accuracy. We note that for a larger model space, the $m_u + m_d$ required to reproduce m_π becomes smaller.

Typical results for the pionic wave function are presented in table 1 in terms of the amplitudes X and Y.

$(\alpha\beta)$	$E_{\alpha\beta}$ (MeV)	$X_{\alpha\beta}$	$Y_{\alpha\beta}$	$X_{\alpha\beta}^2 - Y_{\alpha\beta}^2$
$(1s_{1/2})$	645	0.77	0.49	0.35
$(1p_{1/2})$	959	1.00	0.74	0.45
$(1p_{1/2})$	1108	0.69	0.53	0.20

Table 1: Amplitudes X and Y obtained with $M(r) = cr^3$, $c = 1.25 \text{ GeV fm}^{-3}$ and $m_u + m_d = 36 \text{ MeV}$. The resulting pion mass is $m_\pi = 140 \text{ MeV}$. The normalization is $\sum (X^2 - Y^2) = 1$.

It should be noted that the appearance of the amplitudes Y implies that $(3q\bar{3}\bar{q}), (5q\bar{5}\bar{q})\dots$ components are present in the wave function in addition to $q\bar{q}$ -components. The situation here is analogous to strong ground state correlations in the RPA description of low-lying collective modes in many-body systems (see Fig. 2). This analogy is in fact quite far-reaching. The self-consistent calculation of the confining mean field $M(r)$ corres-

ponds to the Hartree-Fock approximation for each individual quark (inside the hadron) interacting with the Dirac sea. On top of this there exists an additional residual interaction in $q\bar{q}$ -channels, analogous to that operating in particle-hole excitation channels in many-Fermion systems. The point is that chiral symmetry implies a very direct relationship between the scalar interaction generating the confining potential and the pseudoscalar-isovector residual interaction acting selectively in the pion channel.

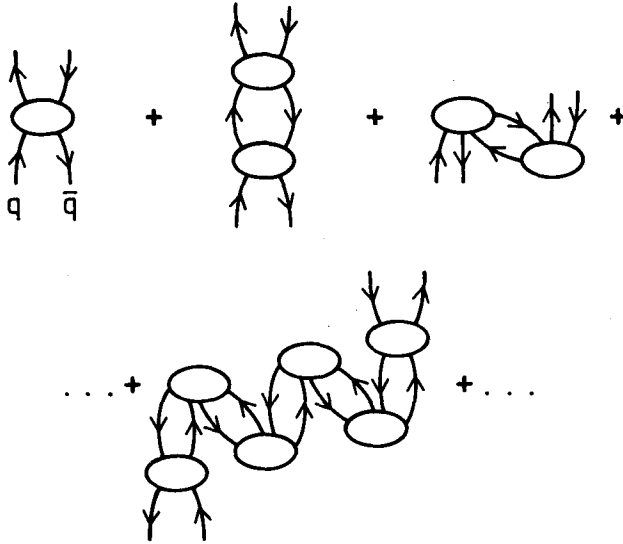


Figure 2: Illustration of the appearance of many-quark-many-antiquark configurations in the pion wave function by the RPA procedure described in the text.

To illustrate this further, we show in Fig. 3 the strength distribution of pseudo-scalar-isovector states which measures the response with respect to an operator $\hat{O} = \int d^3x \bar{\Psi} i\gamma_5 \tau_3 \Psi$. The strength function is $S_N = |\langle O | \hat{O} | \pi_N \rangle|^2$, which satisfies an energy weighted sum rule. The collectivity of the pionic mode becomes obvious again by comparison of RPA and unperturbed strength distributions. Turning on the pseudo-scalar-isovector residual $q\bar{q}$ interaction removes the $J^\pi = 0^-, I = 1$ strength almost completely from the unperturbed states and concentrates it in just one dominant low-lying state, the physical pion. An immediate consequence of this result is that, besides the pion, very little pseudo-scalar-isovector strength should be observable in the meson spectrum at higher masses.

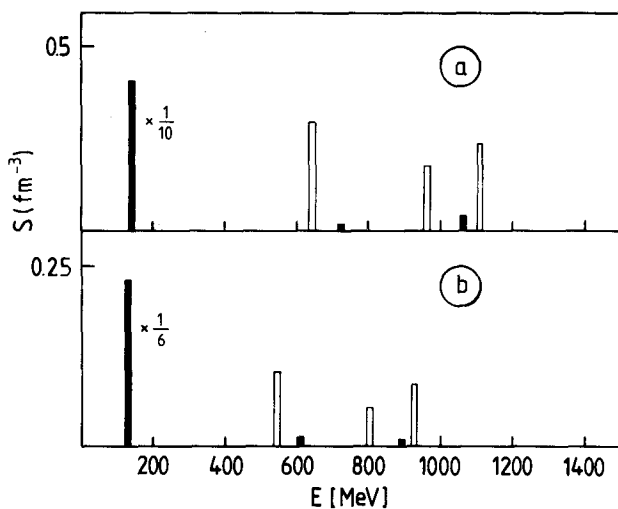


Figure 3: Strength distribution of pionic $q\bar{q}$ -states. The model space is $\{1s_{1/2} \ 1p_{3/2} \ 1p_{1/2}\}$, and a confining potential $M(r) = cr^3$ is used. Upper part (a): $c = 1.25 \text{ GeV fm}^{-3}$; lower part (b): $c = 625 \text{ MeV fm}^{-3}$. Open bars: unperturbed pionic $q\bar{q}$ states (no residual interaction). Solid bars: full RPA calculation with $m_u + m_d = 40 \text{ MeV}$ (see text).

7. Pion Size and Pion Decay Constant

Given the pion wave function of eq. (19) one can calculate the pion rms radius $r_\pi \equiv \langle r^2 \rangle^{1/2}$ and the pion decay constant f_π . The rms radius of the $q\bar{q}$ -core of the pion can readily be expressed in terms of the amplitudes X and Y . The numerical value depends on the size parameter c ; for example, for the value $c = 1.25 \text{ GeV fm}^{-3}$ used in fig. 1 one obtains $r_\pi = 0.46 \text{ fm}$.

The relationship between the radius and the pion decay constant is of some interest. In terms of the amplitudes X and Y the pion decay constant becomes (with $\tilde{g} = g/r$, $\tilde{f} = f/r$):

$$f_\pi = \left[\sqrt{\frac{3N}{2m}} \cos \theta_c / 4\pi \right] \sum_{\alpha\beta} (X_{\alpha\beta} - Y_{\alpha\beta}) \sqrt{2j_\alpha + 1} [\tilde{g}_\alpha(o) \tilde{g}_\beta(o) + \tilde{f}_\alpha(o) \tilde{f}_\beta(o)] \quad (21)$$

where θ_c is the Cabbibo angle, N is a wave function normalization constant, and \tilde{g} and \tilde{f} are the upper and lower components of the spinors u or v (eq. (10)), respectively.

It turns out that f_π is practically independent of the quark masses as long as $m_u + m_d \ll E_\alpha$, as expected; f_π depends, however, rather sensitively on the size parameter and therefore on the pion radius. In fig. 4 the connection between r_π and f_π is shown graphically. The experimental value $f_\pi = 93 \text{ MeV}$ is reproduced for $r_\pi = 0.43 \text{ fm}$. This is not unreasonable, since r_π should be smaller than the measured charge radius of the pion, with additional contributions to the charge density presumably coming from meson cloud effects not included in the model. The fact that f_π can be made compatible with a rather small core size of the pion is due to the high degree of collectivity of the pion wave function. This is demonstrated in Fig. 4 by

comparison with a "standard" model where the pion is a single $q\bar{q}$ pair in a pure $(1s\ 1/2)^2$ configuration.

The result obtained for f_π follows very closely an inverse proportionality, $f_\pi = \text{const}/r_\pi$. The constant is related to the "spectroscopic factor" Z for finding a $q\bar{q}$ pair in the pion, $|\pi\rangle = \sqrt{Z}|q\bar{q}\rangle + \dots$ etc. Brodsky and Lepage¹⁰⁾, in their analysis of $\pi \rightarrow \mu\nu$ and $\pi^0 \rightarrow 2\gamma$ decays, obtain phenomenological values $r_\pi = 0.42$ fm and $Z \lesssim 1/4$. Our radius turns out to be very close to that of ref. 10). While our Z factor cannot be directly compared with theirs, we nevertheless find a value close to their upper limit. Again, in the present model the greatly reduced $q\bar{q}$ -valence pair content of the pion is a necessary consequence of the collectivity of the pion mode. The spectroscopic factor will be further reduced by couplings e.g. to $2q2\bar{q}$ states not included in RPA. Consequently, we expect also that r_π given here is probably an upper limit.

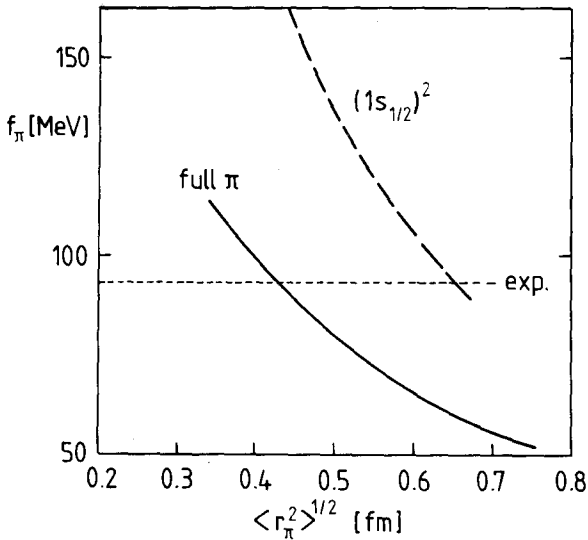


Figure 4: Dependence of the pion decay constant f_π on the rms radius of the pion core. Dashed curve: $q\bar{q}$ -pion in pure $(1s\ 1/2)^2$ configuration. Solid curve: "collective" pion, represented by the amplitudes X and Y in a $\{1s, 1p\}$ model space (see also table 1). The full curve is very well approximated by $f_\pi = 0.2/r_\pi$.

8. Related topics

8.1 Pion cloud contributions to the proton charge form factor

The finite pion size provides a natural cutoff in calculations of the nucleon self-energy due to pion cloud effects, as shown in Fig. 5. While this procedure diverges for pointlike pion-quark coupling vertices in chiral bag models, it gives meaningful results if the pion has a finite radius.

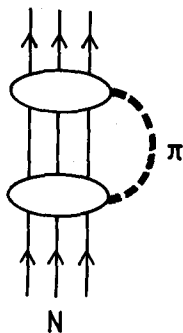


Figure 5: Nucleon self-energy due to the dressing of the three-quark core by a pion cloud.

The pion cloud contributes to the nucleon charge distribution. We show here a calculation ¹¹⁾ of the proton charge form factor which has been performed as follows: the three valence quarks are assumed to move in a confining potential $M(r) = cr^3$. The wave functions are projected onto fixed total momentum, as in refs. 7,8). A chiral pion quark coupling is introduced as in ref. 8), but with a Gaussian momentum space cutoff reflecting the finite size of the pion and adjusted to an rms radius of 0.4 fm. To obtain the charge form factor, a virtual photon is coupled, in a gauge invariant way, to any quark or charged pion line in Fig. 5. The procedure includes the ρ -meson pole structure of the $\gamma\pi\pi$ form factor. The summation over all intermediate three-quarks states turns out to be terminated by the finite pion size in such a way that it involves essentially N and Δ intermediate states, times a charge renormalization factor.

The result is shown in Fig. 6. For a pion radius of 0.4 fm, the pion cloud carries about 1/3 of the proton charge, while 2/3 remain in the three-quark core. The proton charge radius is in large part determined by the pion cloud, while at larger momentum transfers, the valence quark core starts to dominate, as expected. Also shown in Fig. 6 for comparison is the standard dipole fit, $G_E = (1 - q^2/0.71 \text{ GeV}^2)^{-2}$.

7.2 Nucleon Axial form factor

It is useful to consider the axial form factor $G_A(q^2)$ (the Fourier transform of $A_3^3(x)$, see eq. (2) together with the charge form factor $G_E(q^2)$. The axial form factor measures essentially the spin distribution within the nucleon. The role of the pion field in $G_A(q^2)$ differs substantially from that in $G_E(q^2)$. In fact, the leading terms in the axial current to first order in the pion field, $f_\pi \partial^\mu \phi_\pi$, do not contribute to $G_A(q^2)$ at all as long as ϕ_π is a continuous function of position relative to the nucleon center-of-mass. To that order, $G_A(q^2)$ is entirely determined by the three-quark valence core ⁸⁾.

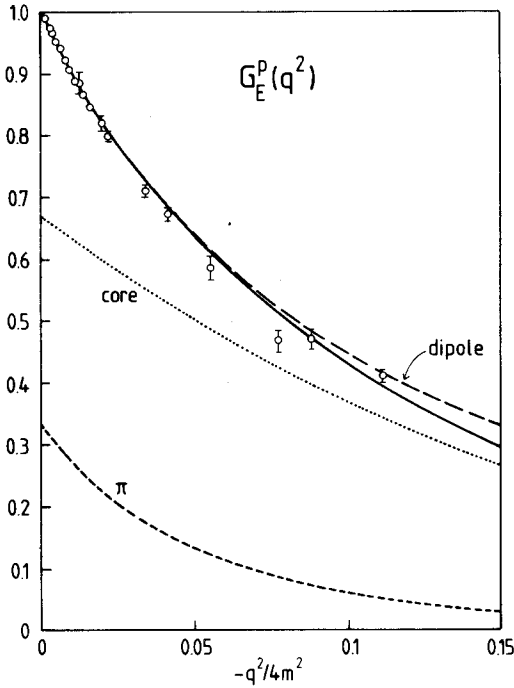
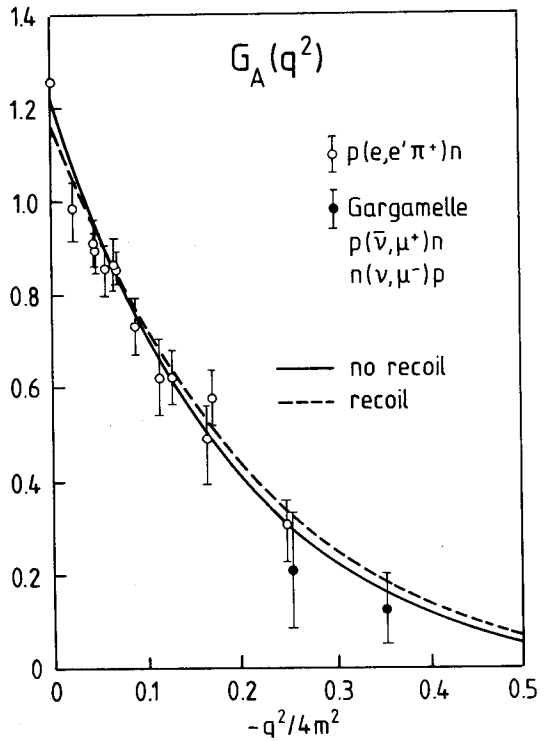


Figure 6:
 Proton charge form factor showing separately the contributions from the three-quark valence core and from the coupling of the virtual photon to the pion cloud. (Input: confining potential $M(r)=cr^3$ with $\langle r^2 \rangle^{1/2}=0.55$ fm for the quark core; Gaussian pion-quark vertex with radius $r_\pi=0.4$ fm.) The resulting proton charge radius is $\langle r_p^2 \rangle^{1/2}=0.83$ fm (m is the nucleon mass).

Figure 7:
 The nucleon axial form factor calculated according to ref. 8) from the three-quark valence core alone. The input is the same as in $G_E(q^2)$. Here m is the nucleon mass. The solid curve: no recoil corrections; dashed curve: recoil corrections included according to the projection procedure described in ref. 8).



The result for $G_A(q^2)$ using the same quark-core input as in $G_E(q^2)$ is shown in Fig. 7. The degree of consistency between G_E and G_A is remarkable, but one should note that refinements may be necessary if terms non-linear in the pion field are added. The normalization of the axial form factor is $G_A(0) = g_A$, the axial charge, the empirical value being $g_A = 1.26$. The pion-nucleon coupling constant is

$$g_{\pi NN} = G_{\pi NN}(q^2 = m_\pi^2), \quad (22)$$

where $G_{\pi NN}(q^2)$ is the pion-nucleon form factor which is related, at $q^2 = 0$, to g_A by the Goldberger-Treiman relation

$$G_{\pi NN}(0) = \frac{m}{f_\pi} g_A. \quad (23)$$

The size associated with $G_A(q^2)$ implies a relatively soft $G_{\pi NN}(q^2)$ (8,12). In fact, $G_{\pi NN}$ is well approximated by an exponential,

$$G_{\pi NN}(q^2) = G_{\pi NN}(0) \exp [q^2/\Lambda^2], \quad (24)$$

Using the same quark core wave functions as those determining the axial form factor, Fig. 7, one obtains $\Lambda \approx 0.7$ GeV. Such an extended πN -vertex has to be confronted with the much shorter ranged cutoffs usually employed in phenomenological one-boson exchange models of the NN interaction.

References:

- 1) A. Chodos and C.B. Thorn, *Phys. Rev. D* 12 (1975) 2733
- 2) G.E. Brown and M. Rho, *Phys. Lett.* 82 B (1979) 177;
G.E. Brown, M. Rho and V. Vento, *Phys. Lett.* 84 B (1979) 383;
V. Vento, M. Rho, E. Nyman, J.H. Jun and G.E. Brown,
Nucl. Phys. A 345 (1980) 413
- 3) G.A. Miller, A.W. Thomas and S. Th  berge, *Phys. Lett.* 91 B (1980) 192;
S. Th  berge, A.W. Thomas and G.E. Miller,
Phys. Rev. D 22 (1980) 2838, *Phys. Rev. D* 24 (1981) 216;
- 4) Y. Nambu and G. Jona-Lasinio
Phys. Rev. 122 (1961) 345, *Phys. Rev.* 124 (1962) 246
- 5) R. Brockmann, W. Weise and E. Werner, *Phys. Lett.* 122 B (1983) 201;
W. Weise, in: *Quarks, Mesons and Isobars in Nuclei*,
R. Guardiola and A. Polls, eds., World Scientific (1983), p. 146;
- 6) V. Bernard, R. Brockmann, M. Schaden, W. Weise and E. Werner,
Nucl. Phys. A (1983), in print
- 7) R. Tegen, R. Brockmann and W. Weise, *Z. Physik A* 307 (1982) 339
- 8) R. Tegen, M. Schedl and W. Weise, *Phys. Lett.* 125 B (1983) 9;
R. Tegen and W. Weise, *Z. Physik A* (1983) in print
- 9) M.A. Shifman, A.I. Vainshtein and V.I. Zakharov,
Nucl. Phys. B 147 (1979) 385, *Nucl. Phys. B* 163 (1980) 43
- 10) S.J. Brodsky, in: *Quarks and Nuclear Forces*,
Springer Tracts in Mod. Phys. 100 (1982) 81;
S.J. Brodsky and G.P. Lepage, *Phys. Scripta* 23 (1981) 945
- 11) E. Oset, R. Tegen and W. Weise, preprint (1983)
- 12) P.A.M. Guichon, G.A. Miller and A.W. Thomas, *Phys. Lett.* 124 B (1983) 109